Regular Article

INORGANIC CHEMISTRY RESEARCH
Published by the
Iranian Chemical Society
www.inorgchemres.org
info@inorgchemres.org

Inorg. Chem. Res., *Vol. 5, No. 1, 82-93, June 2021*
DOI: 10.22036/icr.2021.238089.1076

Palladium Supported on Schiff Base Functionalized Magnetite Nanoparticles as an Efficient Catalyst for Coupling Reactions

Masomeh Balali[a], Mojtaba Bagherzadeh[b,*], Razieh Nejat[c] and Hassan Keypour[d,*]

[a]*Hamedan University of Technology, 65155 Hamedan, Iran*
[b]*Chemistry Department, Sharif University of Technology, P. O. Box: 11155-3615, Tehran, Iran*
[c]*Faculty of Science, Department of Chemistry, Kosar University of Bojnord, Iran*
[d]*Faculty of Chemistry, Bu-Ali Sina University, Hamedan 65174, Iran*

(Received 5 September 2020, Accepted 3 January 2021)

Palladium has been supported on 2-((3-(piperazin-1-yl) propylimino)methyl)phenol functionalized magnetite nanoparticles (denoted as Fe_3O_4@SiO_2@L-Pd(II)). The supported Pd was used as an active heterogeneous catalyst in the Suzuki cross-coupling reaction under solvent-free conditions. This nanocatalyst could be facilely separated *via* magnetic concentration and the isolated catalyst exhibited long-term stability. Easy work-up, high yield, recycling of the catalyst, low reaction times, non-toxicity of catalyst and solvent-free conditions as an environmentally benign procedure are the main merits of this protocol. The produced catalyst were characterized by XRD, FT-IR, XPS, SEM, TEM, EDAX, VSM, TGA and ICP-OES.

Keywords: Palladium catalyst, Suzuki reaction, Magnetic separation, Solvent-free conditions

INTRODUCTION

Palladium nanoparticles as noble metal nanoparticles due to their ultrafine sizes and large surface area, play an important role for catalytic application in organic reactions such as in Stille Suzuki, Heck and Sonogashira coupling reactions [1-4]. On the other hand, palladium high cost and limited world supply hinder their application in wide scale. Hence, in order to improve their catalytic properties and restrict metal nanoparticles agglomeration, several strategies have been developed for design and fabrication catalyst support. However, immobilization and dispersion of Pd complexes onto different carriers with large specific surface areas as recyclable heterogeneous catalysts, has attracted much attention and made great advances. In this context, a series of supporting substrates have been developed for immobilizing Pd catalysts, for example, silica [5-8], carbon material [9-13], mesoporous silica [14-18], dendrimers [19,20], metal oxides [21,22] and polymers, [23-25]. Besides, an applicable strategy for separating of catalyst is use of magnetic nanoparticles (MAGNPs) and so it can be easily separated from the reaction medium using an external permanent magnet. Hence, this separation technique provides an easy separation of the nanocatalysts without the need for centrifugation, filtration or other tedious workup processes [26].

Recently, number of procedures are now recommended for Green Chemistry involving: either new eco-friendly reagents and catalysts, selected media such as water, supercritical fluids, ionic liquids or solvent-free reactions [16].

In this work, we have explored a new Pd-containing magnetically separable system as an efficient catalyst for the Suzuki-Miyaura reaction under solvent-free conditions that design of solventless catalytic reaction has received tremendous attention in recent times in the area of green synthesis.

*Corresponding authors. E-mail: bagherzadeh@sharif.edu; haskey1@yahoo.com

EXPERIMENTAL

General

Tetraethoxysilane (TEOS), 3-choloropropyltriethoxy-silane (CPTES), 3-(piperazin-1-yl)propan-1-amine and 2-hydroxybenzaldehyde were purchased from Aldrich. All other chemicals were of analytical grade and used without further purification.

Characterization Methods

The structure of the new magnetite nanocatalyst was characterized by FT-IR, SEM, EDX, TEM, XRD, TGA, VSM and XPS analysis. ^{1}H NMR and ^{13}C NMR spectra were recorded in $CDCl_3$ using a Bruker Avance 90 MHz instrument (DRX). Melting points were measured with a SMPI apparatus. X-ray diffraction (XRD) measurement was recorded by X-ray diffractometer ITAL STRUCTURES model APD2000 with applying Cu Kα radiation, in at 2θ range of 5°-90°. Morphology and particle dispersion was investigated by scanning electron microscopy (SEM) (Philips XL30). Pd content of the catalyst was determined by inductively coupled plasma-atomic emission spectrometer (ICP-AES). Transmission electron microscopy (TEM) images were performed on an EM10C (Zeiss) transmission electron microscope at an accelerating voltage of 80 kV. Samples dispersed in solution were cast onto a carbon-coated copper grid.

FT-IR spectra was carried out as KBr pellets using a Perkin Elmer Spectrum Version 10.01.00 spectrophotometer. The TGA/DTA curves were performed using 851 Mettler Toledo apparatus. X-ray photoelectron spectroscopy (XPS) was recorded by Dual anode (Mg and Al Kα) a chromatic X-ray source.

Magnetic measurement of materials was carried out with a vibrating sample magnetometer VSM (4 inches, Daghigh Meghnatis Kashan Co., Kashan, Iran) at room temperature.

Preparation of Catalyst

Preparation of 2-((3-(piperazin-1-yl)propyl-imino)methyl)phenol (L). 2-Hydroxybenzaldehyde (0.122 g, 1.00 mmol) in ethanol was added dropwise with stirring to a solution of 3-(piperazin-1-yl)propan-1-amine (0.143 g, 1.00 mmol) in ethanol (50 mL), over a period of 60 min. The mixture was stirred and refluxed for 2 h. A yellow precipitate was obtained that was filtered off and washed with ethanol and dried in vacuum [27]. Yield: 0.220 g (88%). m.p.: 118 °C, IR (KBr, cm^{-1}): 1640 (ν(C=N)) 1596, 1484 ($\nu(C=C)_{ar}$). ^{1}H NMR (90 MHz, $CDCl_3$): δH (ppm): 1.7-3.766 (m, 14H, CH_2), 8.569 (s, H, CH=N), 6.352-7.988 (m, 4H, ArH), 5.353 (s, 1H, OH).

Preparation of Fe_3O_4@SiO_2@L. At first, Fe_3O_4, Fe_3O_4@SiO_2 and Fe_3O_4@SiO_2@Cl magnetic nanoparticles were synthesized according to the procedure previously reported in literature [28-30]. The obtained Fe_3O_4@SiO_2@Cl was sonicated and dispersed separately in dry methanol (20 mL) for 10 min. L (0.8 mmol) was added to above mixture under argon atmosphere.

After stirring under argon at room temperature for 24 h, the resultant solid was separated magnetically, then washed with methanol several times to remove the unreacted residue of the L and dried under vacuum at 303 K for 24 h.

Preparation of palladium catalyst (Fe_3O_4@SiO_2@L-Pd). For the preparation of nanocatalyst, 1.0 g of Fe_3O_4@SiO_2@L nanoparticles was suspended in 100 mL of dry ethanol and then $PdCl_2$ (1.0 mmol) was added to the suspension of nanoparticles and the reaction mixture was refluxed for 24 h under a nitrogen atmosphere. After separation with an external magnet, the product was washed with ethanol several times to remove unreacted L.

Application of Catalyst for Suzuki Reaction

A mixture of aryl halide and phenyl boronic acid, with an equivalent molar ratio of 1.0-1.5, Fe_3O_4@SiO_2@L-Pd catalyst (0.03 g) and K_2CO_3 (2.0 mmol) are placed in a mortar. The reaction mixture was then heated at 100°C for an appropriate time (Table 2) until the completion of the reaction was achieved as monitored by TLC. After completion of the reaction, EtOAc (10 mL) was added to the mixture, stirred for 5 min and filtered to separate the catalyst. Water (15 mL) was added and the products were extracted with ethylacetate (3 × 20 mL). The organic layer was dried over anhydrous Na_2SO_4 and then dried by rotary evaporation. The purification of the resulted crude products by column chromatography

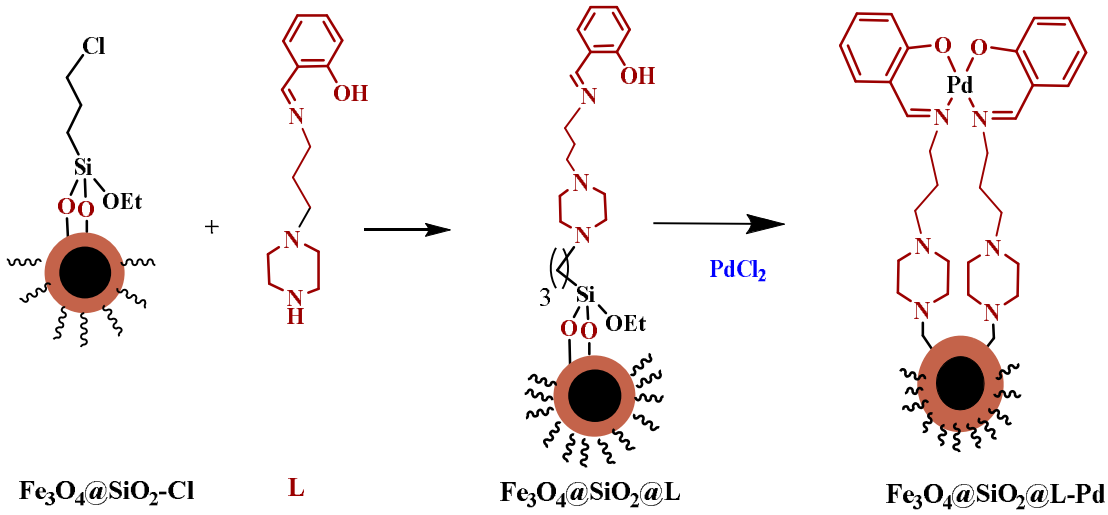

Scheme 1. Step-by-step synthesis of Fe_3O_4@SiO_2@L-Pd

(hexane/ethylacetate) was given the pure products in excellent yields.

RESULTS AND DISCUSSION

Characterization of the Novel Catalyst

The nanocatalyst preparation steps are summarized in Scheme 1. Briefly, Fe_3O_4 nanoparticles were prepared by the co-precipitation method [28]. Next, the surface of Fe_3O_4 was coated with a thin layer of silica using tetraethyl orthosilicate [29].

The presence of a broad band in the IR spectrum around 1091 cm^{-1} (Fig. 1, supporting information) confirmed the formation of the Si-O-Si bonds. The silica coated Fe_3O_4 nanoparticles were allowed to react with 3-chloropropyltriethoxysilane which introduced -Cl group on to the surface of support [30]. In the next step, Fe_3O_4@SiO_2@Cl nanoparticles were reacted with 2-((3-(piperazin-1-yl)propylimino)methyl)phenol (L). The Fe_3O_4@SiO_2@L exhibits a υ(C=N) stretch at 1642 cm^{-1} (Fig. 1b). Next, Fe_3O_4@SiO_2@L was reacted with the palladium (II) chloride in ethanol to synthesize of Fe_3O_4@SiO_2@L-Pd and the absorption of C=N bond in nanocatalyst shifted to a lower wave number (1635 cm^{-1}) after it chelated with Pd ions (Fig. 1C) [31-32].

The compositional analysis has been characterized using EDAX in order to confirm the elements present in Fe_3O_4@SiO_2@L-Pd as catalyst. As shown in Fig. 2a, elements Fe, C, O, Si, N and Pd without other impurities were detected by EDX, suggesting a successful preparation of the Fe_3O_4@SiO_2@L-Pd nanoparticles [33].

XRD pattern of Fe_3O_4 (Fig. 2b) shows six diffraction peaks at 2θ about 30.2, 35.5, 43.1, 53.2, 57.1 and 63.8° which are marked by their indices (220), (311), (400), (422), (511) and (440), respectively [34]. The broad peak at 2θ = 20-29° is assigned to the amorphous silica, indicating that the silica was successfully coated on the surface of Fe_3O_4 nanoparticles.

The results for Fe_3O_4@SiO_2@L-Pd are in agreement with standard patterns of inverse cubic spinel magnetite (Fe_3O_4). The peak intensity is weakened and its width is broadened gradually in Fe_3O_4@SiO_2@L-Pd (Fig. 2b).

The Fe_3O_4@SiO_2@L-Pd(II) catalyst involved Pd(II) rather than Pd (0), therefore its main peaks were similar to the Fe_3O_4@SiO_2 and did not show the characteristic peak of Pd (as shown in Fig. 2b) [35].

Furthermore, the Palladium content of the nanoparticle was carried out by the inductively coupled plasma optical emission spectroscopy (ICP/OES) analysis to be about 0.7 mmol g^{-1}.

Figures 3a and 3b presents X-ray photoelectron spectroscopy (XPS) elemental survey scans of the surface

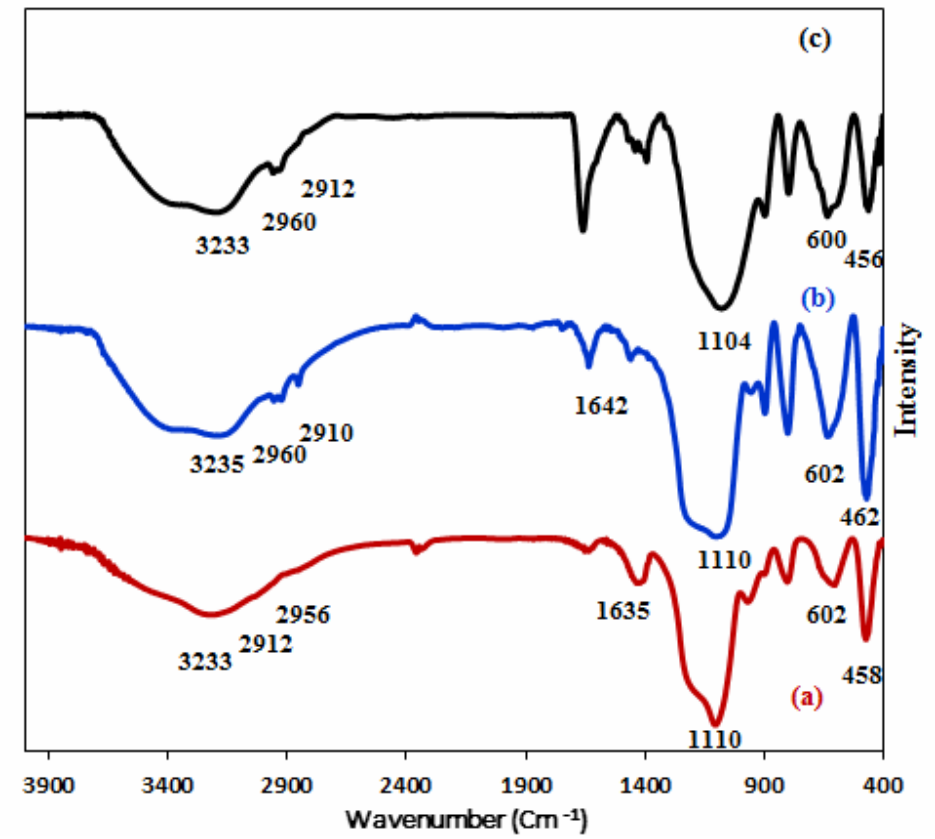

Fig. 1. FT-IR spectra of (a) Fe_3O_4@SiO_2@Cl, (b) Fe_3O_4@SiO_2@L and (c) Fe_3O_4@SiO_2@L-Pd catalyst.

and the Pd binding energy of the Fe_3O_4@SiO_2@L-Pd catalyst, respectively.

XPS analysis of the Fe_3O_4@SiO_2@L-Pd nanoparticles (Fig. 3a) shows expected elements on the surface of nanocatalyst such O, C, N and Pd. The XPS spectrum of Pd 3d (Fig. 3b) can be fitted to two strong peaks at BE of 342.88 and 337.88 eV, which are assigned to Pd 3d3/2 and Pd 3d5/2, respectively. These values agreed with the oxidation state (+2) of Pd. In addition, a weak shoulder peak appears at 336.4 eV (Pd 3d5/2), suggesting the Pd(0) exists on the surface of the catalyst [36].

Transmission electron microscopy (TEM) and scanning electron microscopy (SEM) were employed to characterize the micromorphology and the size and shape of nanoparticles. As shown in the SEM images (Fig. 4a), Fe_3O_4@SiO_2@L-Pd nanocatalysts were present as uniform particles with spherical morphology). From the TEM micrographs, average particle size of Fe_3O_4@SiO_2@L-Pd nanoparticles is estimated between 40 to 50 nm. [37]

TGA studies were carried out for Fe_3O_4@SiO_2@L-Pd nanoparticles to determine the content of organic functional groups of the sample (Fig. 5). TGA experiments were measured under nitrogen atmosphere with a heating rate of 10 ºC per minute in the temperature range 25-600 ºC.

The TGA curve of nanoparticles, that of Fe_3O_4@SiO_2@L-Pd shows the multistep mass loss of the organic materials as a function of temperature. The weight loss in the TGA curve indicated the loss of organic Schiff base and propyl linkage [38] in the sample. At 600 ºC, the residual mass percent of Fe_3O_4@SiO_2@L-Pd is about 77.9%.

Figures 6a and b shows the magnetization of Fe_3O_4@SiO_2 and Fe_3O_4@SiO_2@L-Pd of the applied

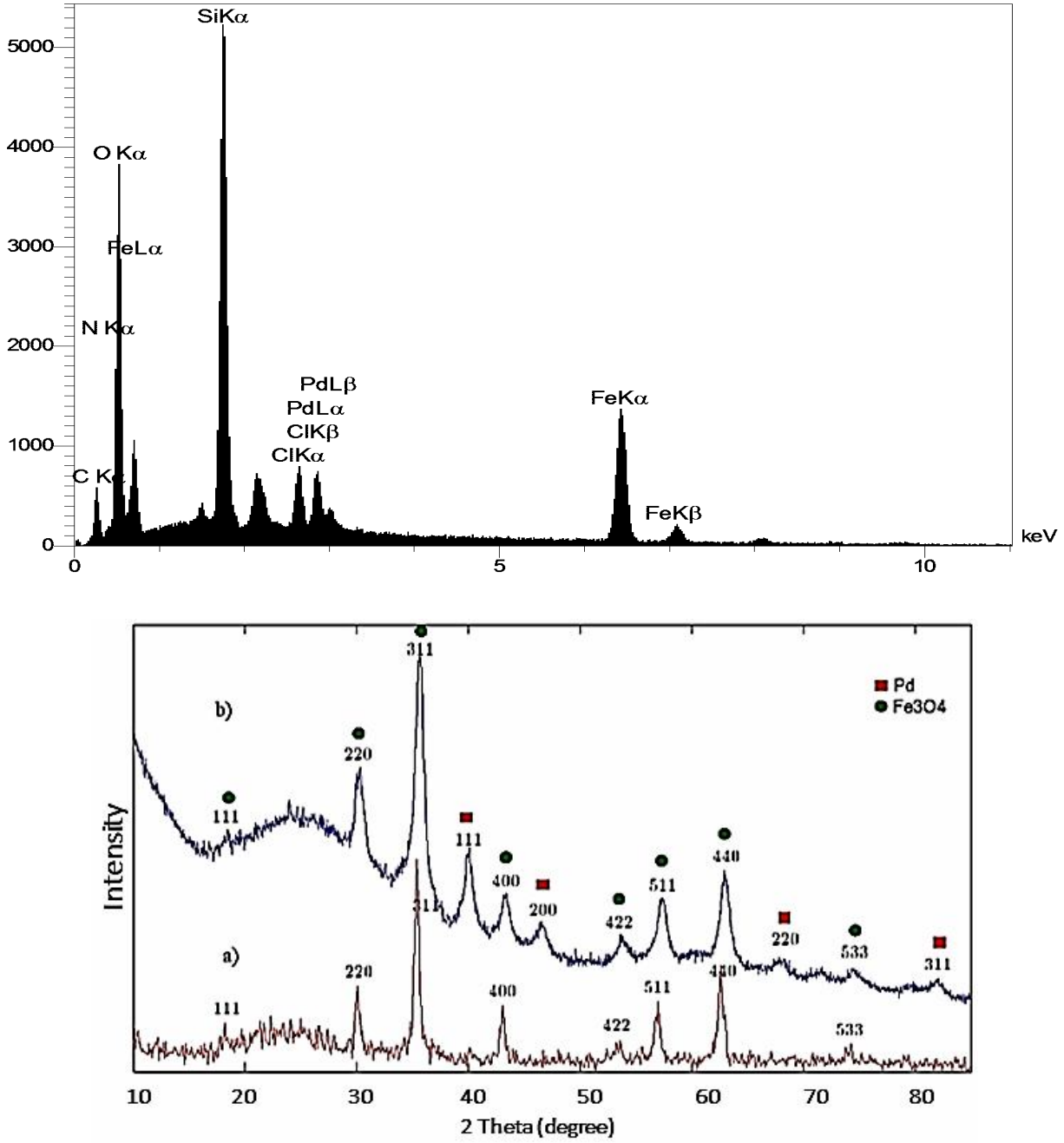

Fig. 2. (a) The energy-dispersive X-ray spectroscopy (EDX) of the Fe_3O_4@SiO_2@L-Pd catalyst. (b) XRD patterns of: a) Fe_3O_4, and b) Fe_3O_4@SiO_2@L-Pd.

magnetic field at 298 K, respectively. Magnetization increased with an increase in the magnetic field. The magnetic saturation values of the two samples are 20.0 and 10.8 emu g^{-1}, respectively. This drop in saturation magnetization value is due to the modification of the Pd(II) complex on the surface of the magnetic supports [39].

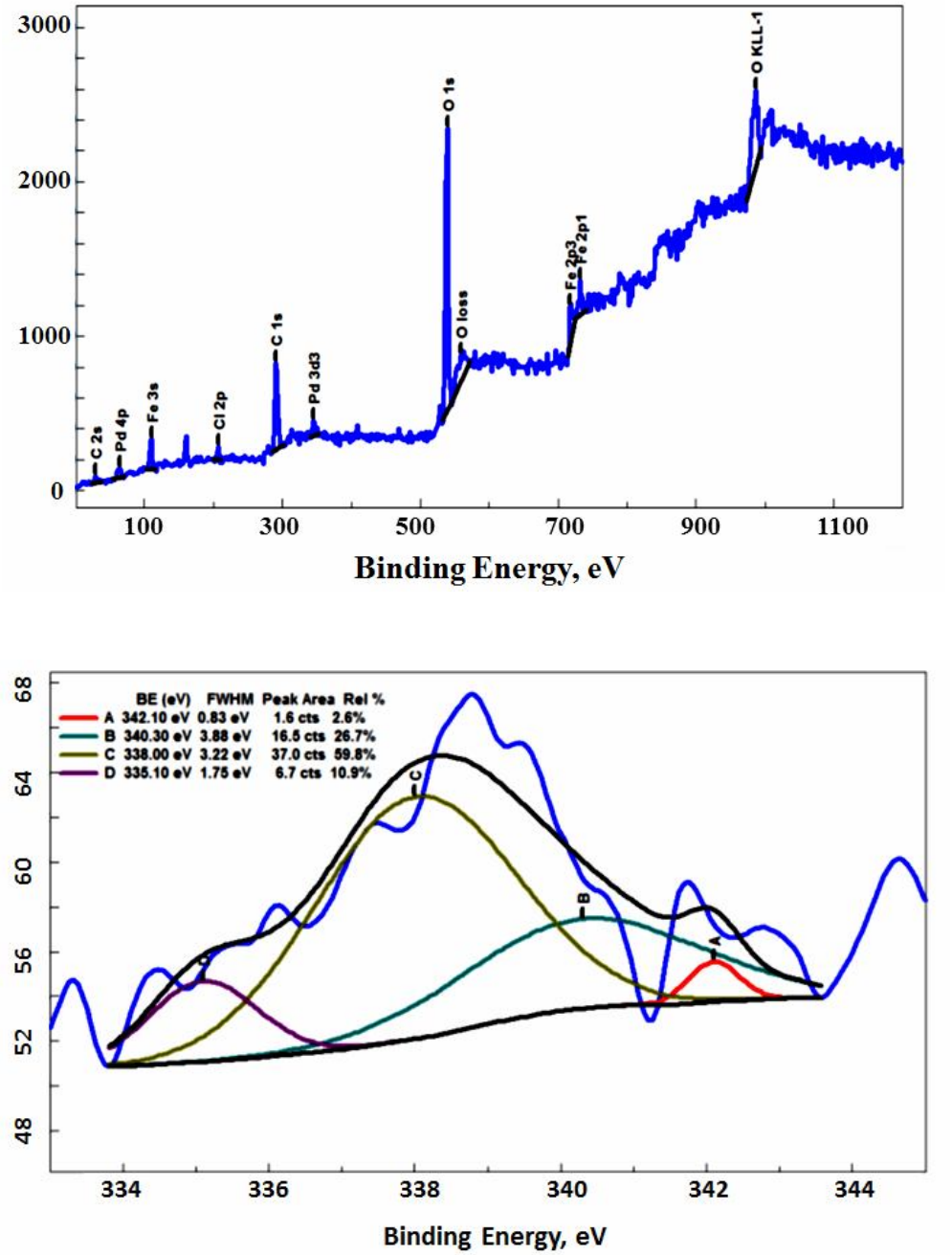

Fig. 3. (a) XPS spectrum of the elemental survey scan of Fe_3O_4@SiO_2@L-Pd and (b) high resolution XPS spectrum of the Fe_3O_4@SiO_2@L-Pd for Pd 3d.

Therefore, the abovementioned result indicated that the Fe_3O_4@SiO_2@L-Pd catalyst separated and recycled from the solution by applying an external magnetic force.

Suzuki Cross-coupling Rreaction by Fe_3O_4@SiO_2@L-Pd Catalyst

The catalytic activity of the Fe_3O_4@SiO_2@L-Pd

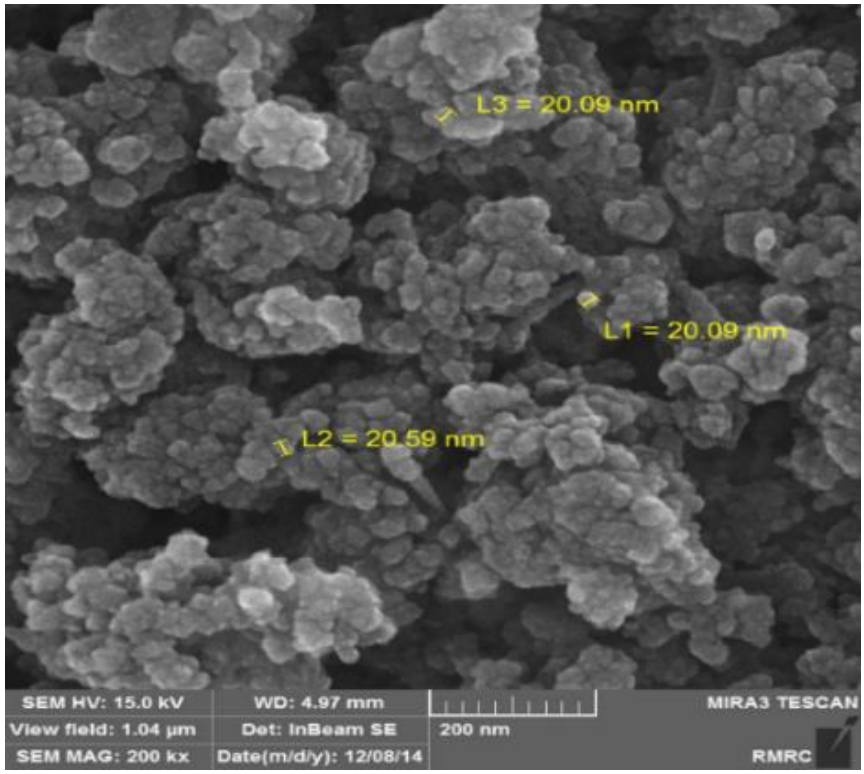

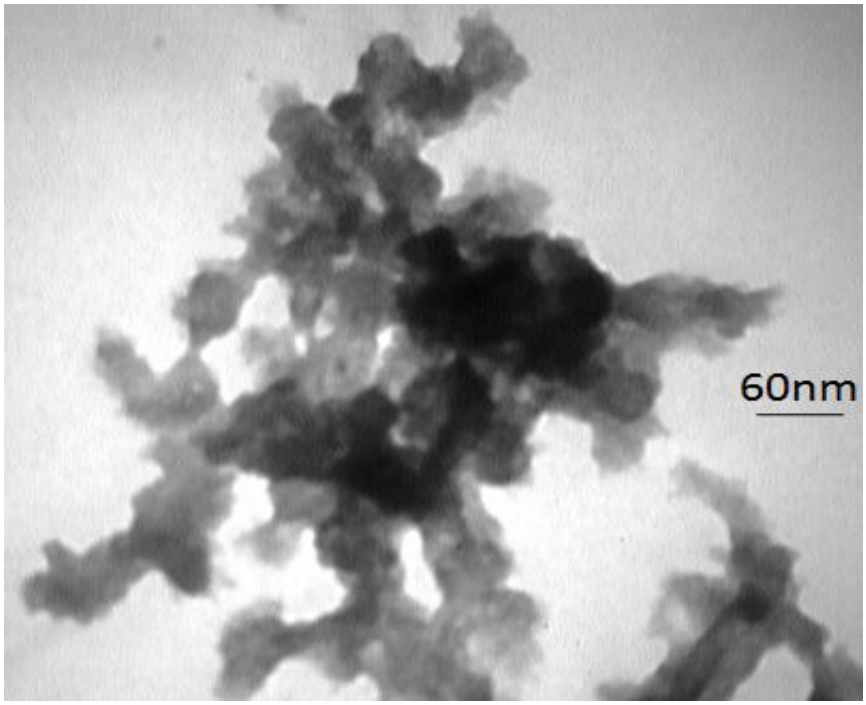

Fig. 4. (a) SEM images of Fe_3O_4@SiO_2@L-Pd nanocatalyst. (b) TEM images of Fe_3O_4@SiO_2@L-Pd nanocatalyst.

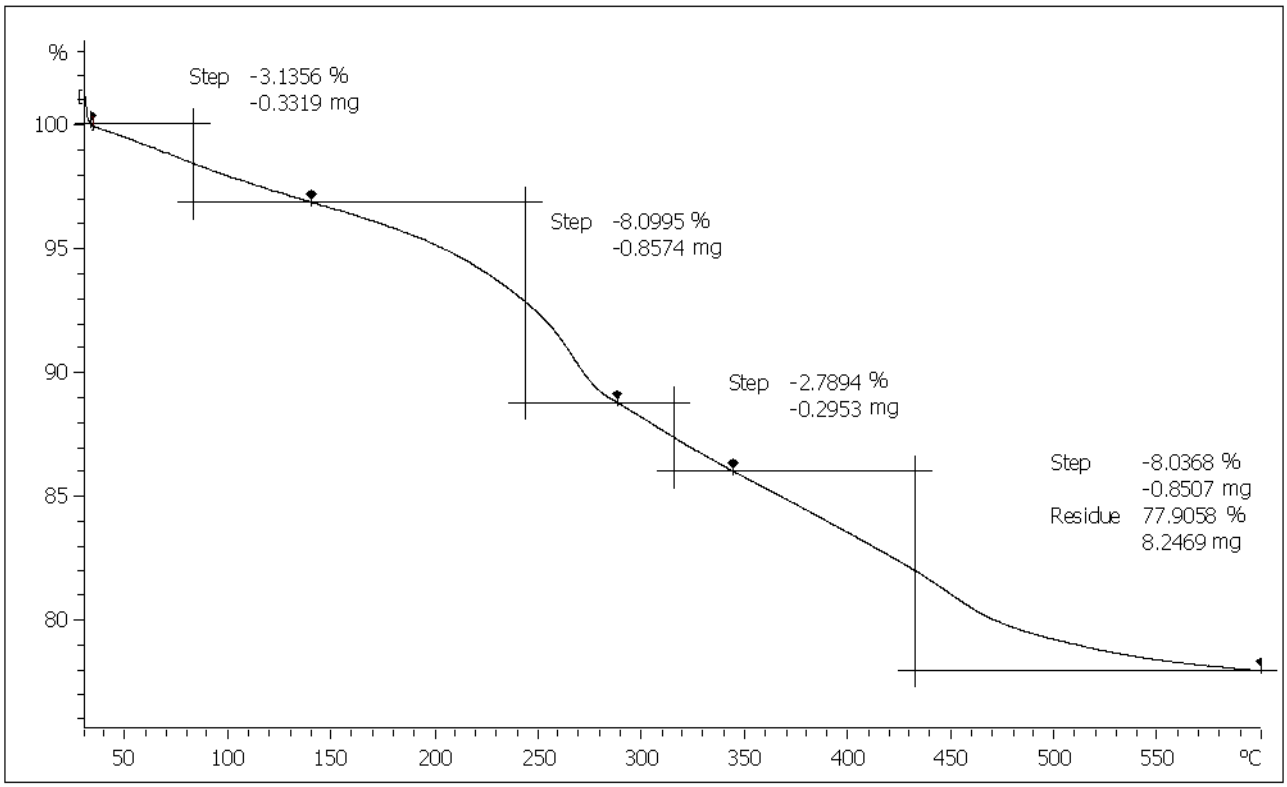

Fig. 5. The TGA analysis of Fe_3O_4@SiO_2@L-Pd catalyst.

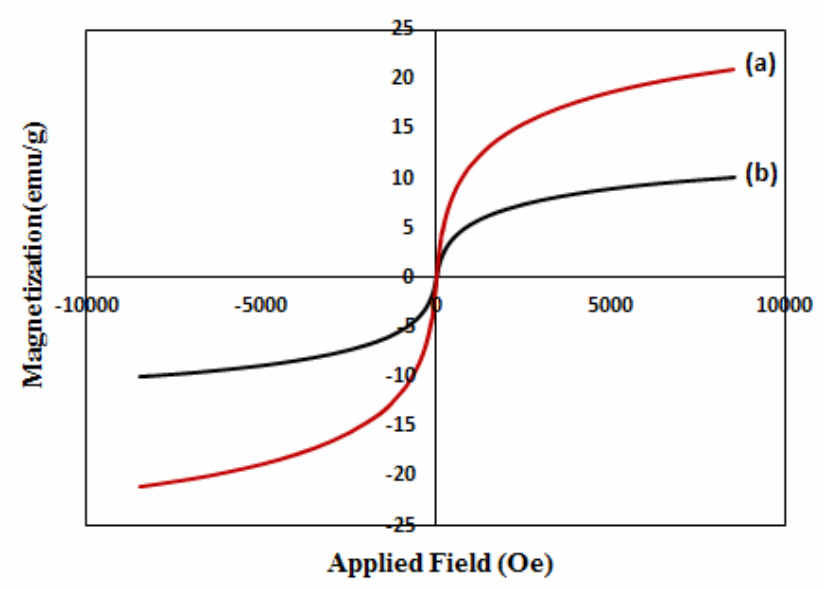

Fig. 6. The VSM analysis of (a) Fe_3O_4@SiO_2 and (b) Fe_3O_4@SiO_2@L-Pd.

Table 1. Optimization Conditions in Suzuki Reaction between Bromobenzene and Phenylboronic Acid in the Presence of Fe_3O_4@SiO_2@L-Pd

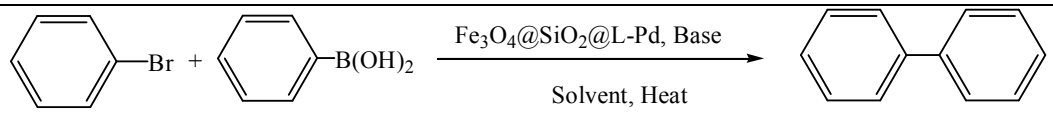

Solvent	Base	Cat. (g)	T (°C)	Time (h)	Yield (%)[a]
None	-	0.03	100	24	-
DMF	K_2CO_3	0.03	100	1	80
H_2O	K_2CO_3	0.03	100	1	55
H_2O	K_2CO_3	0.03	80	1	48
H_2O/H_2O	K_2CO_3	0.03	100	1	80
None	K_2CO_3	0.03	80	1	70
None	K_2CO_3	0.02	100	1	75
None	K_2CO_3	0.03	100	1	90
None	K_2CO_3	0.05	100	1	90
None	NaOH	0.03	100	2	83
None	Et_3N	0.03	100	2	40
None	KOAc	0.03	100	2	65
None	DABCO	0.03	100	2	60

[a]Isolated yield.

catalyst was investigated using the Suzuki cross coupling reaction of bromobenzene and phenylboronic acid in various solvents, catalyst concentrations and bases (Table 1). As shown in Table 1, the best yields were observed in solvent-free conditions and K_2CO_3 as base.

Based on above observations, we investigated the Suzuki cross coupling reaction using various aryl halides and arylboronic acids which results are summarized in Table 2. It is noteworthy that even after five successive usages, the Fe_3O_4@SiO_2@L-Pd nanoparticle retained its catalytic activity as well as its magnetic property.

The stability and recoverability experiments are performed for Suzuki reaction of bromobenzene and phenylboronic acid under optimized conditions (Fig. 7). After separating the catalyst from the reaction, it was washed with deionized ethanol, dried and then directly carried forward to the next reaction. As shown in Fig. 7, it was noticed that the recovered catalyst was recycling in subsequent runs without observation significant decrease in activity even after fifth run.

Table 2. Suzuki Reaction of Aryl Boronic Acids with Aryl Halides[a]

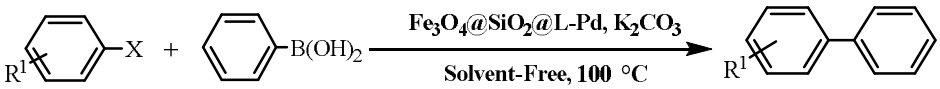

Entry	Ar^1X	Boronic acid	Time (min)	Yield (%)[b]	TON[c]
1	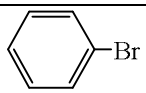	$PhB(OH)_2$	60	90	64.28
2	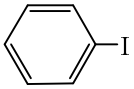	$PhB(OH)_2$	70	87	64.28
3		$PhB(OH)_2$	70	87	62.14
4	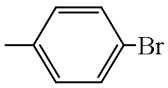	$PhB(OH)_2$	65	80	57.14
5	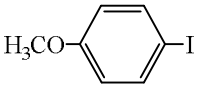	$PhB(OH)_2$	60	85	60.71
6	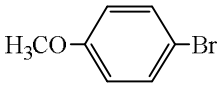	$PhB(OH)_2$	120	88	62.85
7	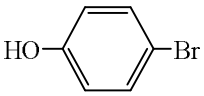	$PhB(OH)_2$	140	78	50
8	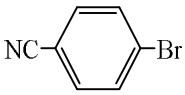	$PhB(OH)_2$	40	91	65
9	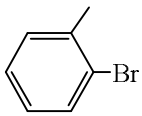	$PhB(OH)_2$	80	86	61.42

[a]Reaction condition: Fe_3O_4@SiO_2@L-Pd, (0.03 g), aryl halide (1 mmol), phenyl boronic acid (1.5 mmol) and K_2CO_3 (2 mmol) under solvent free conditions. [b]Isolated yield. [c]Turnover number.

CONCLUSIONS

In summary, we have successfully developed a new, efficient, inexpensive and experimentally simple Fe_3O_4@SiO_2@L-Pd catalytic system to catalyze Suzuki cross-coupling reaction. Using this new protocol, aryl halides react effectively with phenylboronic acid to provide the corresponding arylated alkynes in high yields

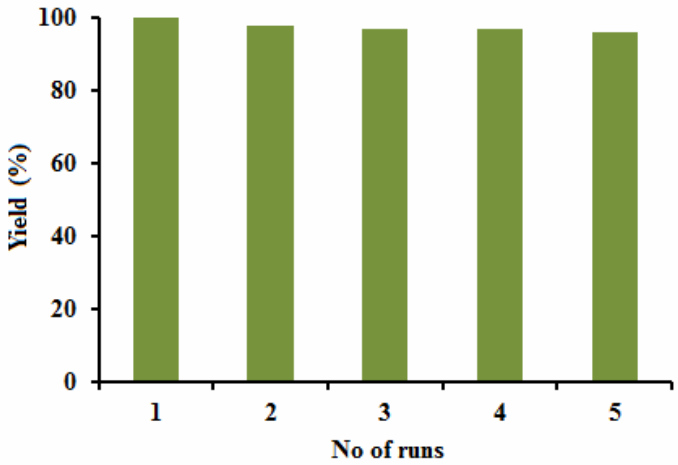

Fig. 7. Results of catalysts reuse experiments in the Suzuki reaction**.**

respectively. Moreover, the nanocatalyst could be completely recovered by magnetic separation from the reaction mixture and showed good activity toward Suzuki cross-coupling reaction in in solvent-free conditions and K_2CO_3 as base. Expectedly, the nanocatalyst can be applied in large-scale industrial synthesis. The complete characterization of catalysts was carried out by means of TGA, SEM, TEM, VSM, XPS and FT-IR.

ACKNOWLEDGEMENTS

We are grateful to the Faculty of Chemistry of Bu-Ali Sina University for financial support. We also acknowledge the Research Council of Sharif University of Technology and Hamedan University of Technology for research funding of this project.

REFERENCES

[1] V. Polshettiwar, C. Len, A. Fihri, Coord. Chem. Rev. 253 (2009) 2599.

[2] F. Alonso, I.P. Beletskaya, M. Yus, Tetrahedron 61 (2005) 11771.

[3] H. Keypour, M. Balali, R. Nejat, M. Bagherzadeh, Appl. Organometal. Chem. 31 (2017) e3691.

[4] T. Azadbakht, M.A. Zolfigol, R. Azadbakht, V. Khakyzadeh, D.M. Perrin, New J. Chem. 39 (2015) 439.

[5] P. Han, X.M. Wang, X.P. Qiu, X.L. Ji, L.X. Gao, J. Mol. Catal. A: Chem. 272 (2007) 136.

[6] Z.L. Zheng, H.F. Li, T.F. Liu, R. Cao, J. Catal. 270 (2010) 268.

[7] D.D. Das, A. Sayari, J. Catal. 246 (2007) 60.

[8] M.A. Zolfigol, T. Azadbakht, V. Khakyzadeh, R. Nejat Yami, D.M. Perrin, RSC Adv. 4 (2014) 40036.

[9] V. Sridhar, H.-J. Kim, J.-H. Jung, C. Lee, S. Park, I.-K. Oh, ACS Nano 6 (2012) 10562.

[10] Z. Zhang, T. Sun, C. Chen, F. Xiao, Z. Gong, S. Wang, ACS Appl. Materials & Interfaces 6 (2014) 21035.

[11] Y. Zhao, L. Zhan, J. Tian, S. Nie, Z. Ning, Electrochim. Acta 56 (2011) 1967.

[12] M. Tanhaei, A. Mahjoub, R. Nejat, Catal. Lett. 148 (2018) 1549

[13] G.M. Scheuermann, L. Rumi, P. Steurer, W. Bannwarth, R. Mulhaupt, J. Am. Chem. Soc. 131 (2009) 8262.

[14] H.H. Wagner, H. Hausmann, W.F.H. olderich, J. Catal. 203 (2001) 150.

[15] H. Ronghua, H. Wenyan, C. Mingzhong, Chin. J. Chem. 29 (2011) 1629.

[16] F. Gao, R. Jin, D. Zhang, Q. Liang, Q. Ye, G. Liu, Green Chem. 15 (2013) 2208.

[17] R. Nejat, A. Mahjoub, Z. Hekmatian, T. Azadbakht, RSC Adv. 5 (2015) 16029.
[18] R. Nejat, M. Chamack, A. Mahjoub, Appl. Organomet. Chem. 31 (2017) 3745.
[19] K.R. Gopidas, J.K. Whitesell, M.A. Fox, Nano Lett. 3 (2003) 1757.
[20] L. Wu, B.L. Li, Y.Y. Huang, H.F. Zhou, Y.M. He, Q.H. Fan, Org. Lett. 8 (2006) 3605.
[21] M.L. Kantam, S. Roy, M. Roy, B. Sreedhar, B.M. Choudary, Adv. Synth. Catal. 347 (2005) 2002.
[22] A. Gniewek, J.J. Ziolkowski, A.M. Trzeciak, M. Zawadzki, H. Grabowska, J. Wrzyszcz, J. Catal. 254 (2008) 121.
[23] R. Najman, J.K. Cho, A.F. Coffey, J.W. Davies, M. Bradley, Chem. Commun. (2007) 5031.
[24] I.P. Beletskaya, A.N. Kashin, I.A. Khotina, A.R. Khokhlov, Synlett. 10 (2008) 1547.
[25] G.W. Wei, W.Q. Zhang, F. Wen, Y. Wang, M.C. Zhang, J. Phys. Chem. C 112 (2008) 10827.
[26] G. Mamba, A. Mishra, Catalysts 6 (2016) 79.
[27] H. Keypour, P. Arzhangi, N. Rahpeyma, M. Rezaeivala, Y. Elerman, O. Büyükgüngör, L. Valencia, H.R. Khavasi, J. Mol. Struct. 977 (2010) 6.
[28] M. Bagherzadeh, M.M. Haghdoost, F. Matlobi-Moghaddam, B. Koushki-Foroushani, S. Sarazdi, E. Payab, J. Coord. Chem. 66 (2013) 3025.
[29] M. Bagherzadeh, M.M. Haghdoost, A. Shahbazirad, J. Coord. Chem. 65 (2012) 591.
[30] A. Rostami, B. Atashkar, D. Moradi, Appl. Catal. A-Gen. 7 (2013) 467.
[31] M.Z. Kassaee, H. Masrouri, F. Movahedi, Appl. Catal. A-Gen. 395 (2011) 28.
[32] M. Esmaeilpour, A.R. Sardariana, J. Javidi, Appl. Catal. A 445 (2012) 359.
[33] H. Keypour, M. Balali, M.M. Haghdoost, M. Bagherzadeh, RSC Adv. 5 (2015) 53349.
[34] X. Du, J. He, J. Zhu, L. Sun, S. An, Appl. Surf. Sci. 258 (2012) 2717.
[35] J. Xu, Z. Cao, X. Liu, H. Zhao, X. Xiao, J. Wu, X. Xu, J.L. Zhou, J. Hazard. Mater. 317 (2016) 656.
[36] X. Sun, Y. Zheng, L. Sun, Q. Lin, H. Su, C. Qi, Nano-Structures & Nano-Objects 5 (2016) 7.
[37] S. Shylesh, J. Schweizer, S. Demeshko, V. Schnemann, S. Ernst, W.R. Thiel, Adv. Synth. Catal. 351 (2009) 1789.
[38] M. Jafarzadeh, I.A. Rahman, C.S. Sipaut, Synth. Met. 162 (2012) 466.
[39] M. Masteri-Farahani, N. Tayyebi, J. Mol. Catal. A: Chem. 348 (2011) 83.